

Scattering of polaritons by point defects in spatially dispersive media*

R. Maddox and D. L. Mills

Department of Physics, University of California, Irvine, California 92664

(Received 25 July 1974)

For a simple model, we study the scattering of a polariton from a static point defect, in the presence of spatial dispersion. The polariton is scattered elastically by the defect, and in analogy with the theory of the reflection of light from the surface of a spatially dispersive medium, there are several final states possible. For example, when the medium is isotropic (the case considered here), an incident transverse polariton scatters into two transverse polariton final states, and into a longitudinal polariton final state upon striking the defect. The contributions to the cross section from these various scattering processes has been evaluated numerically, for a simple model and parameters appropriate to GaP in the infrared.

I. INTRODUCTION

When an electromagnetic wave propagates through a real crystal, it is scattered from its initial direction by any static defects that may be present. In an optically isotropic medium, an electromagnetic wave (polariton) of frequency Ω and wave vector \vec{k} is scattered elastically by a static defect into a final state with frequency Ω , and wave vector \vec{k}' , where $|\vec{k}'| = |\vec{k}|$.

In a spatially dispersive material, the scattering process may be more complex in nature. To illustrate this, in Fig. 1, we present the polariton dispersion relations in a spatially dispersive medium, where the excitation that couples to the dielectric constant has a frequency which decreases as the wave vector increases. An example would be an infrared-active TO phonon in a semiconducting crystal of the zinc-blende structure. If a transverse polariton of frequency Ω and wave vector k_1 (see Fig. 1) propagates through the crystal, a defect may scatter it to a final state of frequency Ω and wave \vec{k}' , where \vec{k}' equals k_1 in magnitude, but differs in direction. However, for a given direction of the scattered wave, the defect may also scatter the polariton into the transversely polarized state with wave vector k_2 , or the longitudinally polarized state with wave vector k_3 , as indicated in Fig. 1. These last two processes are possible only when spatial dispersion is present, since otherwise there are no normal modes of the crystal with frequency Ω other than those whose wave vector equals k_1 in magnitude. There is a direct analogy between the situation just described and the theory of the reflection of light by the surface of a spatially dispersive medium.¹

The purpose of the present paper is to calculate the cross section for the scattering of a polariton from a point defect in a spatially dispersive medium in order to estimate the importance of the scattering into final states of the type k_2 and k_3 in Fig. 1. For this purpose, we employ a simple model which has the virtue of providing reasonably simple expressions for each contribution to the cross sec-

tion.

This calculation is motivated by the experimental work of Evans and Ushioda.² These authors find that the shape and position of the Raman lines associated with the TO and LO phonons observed in backscattering from GaP are quite sensitive to the manner in which the surface is polished. In their paper, Ushioda and Evans argue that the origin of the change in shape and position of the Raman lines lies in the presence of macroscopic strains produced by surface pits present after the polishing process. They form this conclusion after noting that the line shape is altered by an annealing treatment performed after the surface polishing procedure; the effect of annealing is to allow the strains to relax.

But one can also suppose that defects of a microscopic nature are produced by the surface polishing

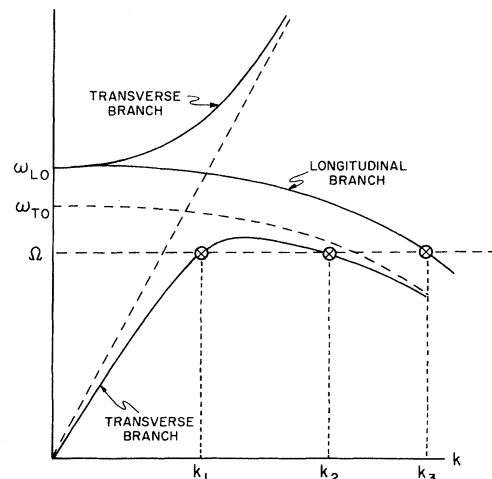


FIG. 1. Dispersion relation for polaritons in a spatially dispersive media, where the infrared-active excitation responsible for the spatial dispersion has a frequency which decreases with increasing wave vector. A static defect in the crystal can scatter a polariton of frequency Ω into final states with wave vector equal in magnitude to k_1 , k_2 , or k_3 .

procedure (atoms displaced from lattice sites into interstitial sites and impurities introduced into the near vicinity of the surface by the polishing and cleaning process). The distribution of defects may be affected by annealing, since they may diffuse during the annealing process. The presence of these defects can scatter a polariton, and thus affect the Raman spectrum. If one estimates the scattering cross section from this process by treating the polariton as a simple electromagnetic wave in a dielectric material, then one expects this scattering to be very weak. [This estimate may be made from Eq. (36) or Eq. (37) below.] We find that for frequencies near ω_{TO} , the fact that spatial dispersion allows scattering into the final states k_2 and k_3 of Fig. 1 leads to an enhancement of the cross section by a very large factor, as large as 10^{10} or 10^{11} . Nonetheless, even when this enhancement is considered, we still find that the scattering cross section is quite small, for infrared frequencies. Thus, even under the most favorable circumstances, it seems difficult to explain the data of Evans and Ushioda by invoking the presence of small-sized defects present near the surface as a consequence of the surface work. Thus, while we show here that spatial-dispersion effects enhance the cross section for scattering of a polariton from a point defect enormously, nonetheless our final conclusion supports the interpretation of the Raman data offered by Evans and Ushioda.

The organization of this paper is as follows. In Sec. II, we define the model, and we derive expressions for the contributions to the scattering cross section described above. In Sec. III we present numerical calculations which show that scattering into final states of the type k_2 and k_3 in Fig. 1 can be very large, so the dominant contribution to the total cross section comes from these processes. That this may be so is clear from phase-space considerations, and our numerical results indicate that in spatially dispersive media, polaritons may be quite strongly scattered by small defects because of the presence of the large wave-vector final states (k_2 and k_3) illustrated in Fig. 1.

II. DERIVATION OF THE CROSS SECTION FOR SCATTERING OF A POLARITON BY A MODEL POINT DEFECT

We wish to consider a crystal of cubic symmetry where in the presence of spatial dispersion, the polariton dispersion relation is similar to that displayed in Fig. 1. This will be the case for a crystal of the NaCl or zinc-blende structure, where the normal mode which couples to the electromagnetic field is the infrared-active TO-phonon branch. Another case of interest is an exciton level, for which the curvature is positive rather than negative, as in Fig. 1. For simplicity we confine our atten-

tion to cubic crystals.

In the absence of spatial dispersion, one considers coupling between the long-wavelength optical displacement \vec{u} of the ions in the unit cell, and the electric field \vec{E} associated with the polariton. One has for the cubic crystal

$$\ddot{\vec{u}} + \omega_{\text{TO}}^2 \vec{u} = (e^*/M) \vec{E} \quad , \quad (1)$$

where M is the reduced mass of the unit cell, and e^* is the Born effective charge. In terms of the electric dipole moment per unit volume $\vec{P} = ne^* \vec{u}$, Eq. (1) becomes

$$\ddot{\vec{P}} + \omega_{\text{TO}}^2 \vec{P} = (ne^*/M) \vec{E} \quad . \quad (2)$$

We introduce the effect of spatial dispersion into Eq. (2) in a phenomenological fashion by adding to the left-hand side the term $\omega_{\text{TO}}^2 \alpha^2 \nabla^2 \vec{P}$, where α^2 is a phenomenological parameter that is the curvature of the TO-phonon branch of the crystal in the long-wavelength limit. Thus, we replace Eq. (2) by

$$\omega_{\text{TO}}^2 \alpha^2 \nabla^2 \vec{P} + \omega_{\text{TO}}^2 \vec{P} + \ddot{\vec{P}} = (ne^*/M) \vec{E} \quad . \quad (3)$$

Consider the normal modes of the crystal generated by Eq. (3) in the approximation that retardation effects are ignored. For the modes of transverse polarization, $\vec{E} = 0$, and the dispersion relation is

$$\omega_{\text{T}}^2(k) = \omega_{\text{TO}}^2 (1 - \alpha^2 k^2) \quad . \quad (4)$$

The physical interpretation of α^2 is clear from this relation. Note that by letting α^2 be negative, a dispersion relation appropriate to excitons is obtained. For the longitudinal modes, $\vec{D} = 0$, and $\vec{E}_{\text{L}} = -4\pi \vec{P}$, a statement true also when retardation is present. The frequency $\omega_{\text{L}}(k)$ for the longitudinal mode of wave vector \vec{k} is found from

$$\omega_{\text{L}}^2(k) = \omega_{\text{P}}^2 + \omega_{\text{T}}^2(k) \quad , \quad (5)$$

where $\omega_{\text{P}}^2 = 4\pi ne^*/M$. The wave-vector and frequency-dependent dielectric constant $\epsilon(k, \Omega)$ for the model is given by

$$\epsilon(k, \Omega) = \epsilon_0 + \omega_{\text{P}}^2 / [\omega_{\text{T}}^2(k) - \Omega^2] \quad , \quad (6)$$

where ϵ_0 is a background dielectric constant, assumed independent of \vec{k} and Ω .

From Eq. (6), we see that spatial dispersion effects enter the model only through the wave vector dependence of $\omega_{\text{T}}(k)$. In reality, the oscillator strengths ω_{P}^2 and ϵ_0 are also wave vector dependent. Our model is reasonable for frequencies Ω close to ω_{TO} , the region of primary concern for many experimental situations, since when Ω is close to ω_{TO} the dominant contribution in the wave vector dependence of $\epsilon(k, \Omega)$ clearly arises from the wave vector dependence of $\omega_{\text{T}}(k)$. Also note that in the model, the curvature of $\omega_{\text{T}}^2(k)$ and $\omega_{\text{L}}^2(k)$ are identical, and $\epsilon(k, \Omega)$ remains isotropic, even for finite \vec{k} . These properties are specific to our particular model.

Even in a cubic crystal the curvature of $\omega_T^2(k)$ and $\omega_L^2(k)$ will differ, and $\epsilon(k, \Omega)$ will be anisotropic at finite \vec{k} . These special properties of our model greatly simplify the algebra in the discussion below, and allow us to characterize the effect of spatial dispersion by introducing only one new parameter. The use of a more complete model should not greatly affect our qualitative conclusions.

If we now consider Maxwell's equations with $\vec{D} = \epsilon_0 \vec{E} + 4\pi \vec{P}$, $\vec{B} = \vec{H}$ and $\rho = \vec{J} = 0$ everywhere, then we find a second relation between \vec{E} and \vec{P} , for waves of frequency Ω :

$$\nabla(\nabla \cdot \vec{E}) - \nabla^2 \vec{E} - (\Omega^2/c^2)\epsilon_0 \vec{E} - (4\pi\Omega^2/c^2)\vec{P} = 0. \quad (7)$$

One may eliminate \vec{P} from Eq. (7) by operating from the left with the operator $(\omega_{TO}^2 - \Omega^2 + \omega_{TO}^2 \alpha^2 \nabla^2)$. If we introduce the parameter

$$K^2 = (1/\alpha^2)(\Omega^2/\omega_{TO}^2 - 1), \quad (8)$$

and write the lattice contribution χ_L to the static electric susceptibility at $\vec{k} = 0$ in the form

$$\chi_L = \omega_P^2/4\pi\omega_{TO}^2, \quad (9)$$

then we have

$$\begin{aligned} (\nabla^2 - K^2) \left(\nabla^2 + \frac{\omega^2}{c^2} \epsilon_0 \right) E_i(\vec{r}) - (\nabla^2 - K^2) \\ \times \sum_j \frac{\partial^2 E_j(\vec{r})}{\partial x_i \partial x_j} + \frac{4\pi\Omega^2 \chi_L}{c^2 \alpha^2} E_i(\vec{r}) = 0. \end{aligned} \quad (10)$$

The result displayed in Eq. (10) applies to a spatially uniform medium. We now presume that a defect in the material may be modeled by presuming that the defective region is characterized by a background dielectric constant $\epsilon_0 + \Delta\epsilon_0$, and a lattice susceptibility $\chi_L + \Delta\chi_L$. For a void in the crystal, $\Delta\epsilon = 1 - \epsilon_0$, and $\Delta\chi_L = -\chi_L$. Thus, in Eq. (10), we let $\epsilon_0 \rightarrow \epsilon_0 + \Delta\epsilon_0(\vec{r})$, $\chi_L \rightarrow \chi_L + \Delta\chi_L(\vec{r})$, and write Eq. (10) in the form

$$\mathcal{G}(\vec{k}\lambda) = -\frac{\Omega^2}{c^2} \frac{\sum_{\vec{q}\lambda'} M(\vec{k}, \vec{q}) \hat{\epsilon}(\vec{k}\lambda) \cdot \hat{\epsilon}(\vec{q}\lambda') \mathcal{G}(\vec{q}\lambda')}{(k^2 + K^2) \{ (1 - \delta_{\lambda, \ell}) k^2 - (\Omega^2/c^2)\epsilon_0 \} + (4\pi\chi_L \Omega^2/\alpha^2 c^2)} \quad (17)$$

where $\delta_{\lambda, \ell}$ is unity when λ refers to the longitudinal branch, and zero when λ refers to the transverse branch.

We may solve Eq. (17) by iterative methods, and by this means we study the scattering of polaritons by an array of defects.

Consider the form assumed by $M(\vec{k}, \vec{q})$ for an array of nonoverlapping defects. Choose a reference point \vec{R}_n within the n th defect. Also suppose that $\Delta\chi_L(\vec{r})$ assumes the constant value $\Delta\chi_L^{(n)}$, and $\Delta\epsilon_0(\vec{r})$ assumes the constant value $\Delta\epsilon_0^{(n)}$ within the n th defect. Then if $\vec{Q} = \vec{q} - \vec{k}$, one may write $M(\vec{k}, \vec{q})$ in the form

$$\begin{aligned} \sum_j L_{ij} E_j(\vec{r}) = -(\Omega^2/c^2) [(\nabla^2 - K^2)\Delta\epsilon_0(\vec{r}) \\ + (4\pi/\alpha^2)\Delta\chi_L(\vec{r})] E_i(\vec{r}), \end{aligned} \quad (11)$$

where L_{ij} is the operator

$$\begin{aligned} L_{ij} = \delta_{ij} \left[(\nabla^2 - K^2) \left(\nabla^2 + \frac{\Omega^2}{c^2} \epsilon_0 \right) + \frac{4\pi\chi_L}{\alpha^2} \frac{\Omega^2}{c^2} \right] \\ - (\nabla^2 - K^2) \frac{\partial^2}{\partial x_i \partial x_j}. \end{aligned} \quad (12)$$

To solve Eq. (12), expand the electric field in an eigenfunction expansion

$$E_i(\vec{r}) = \sum_{\vec{q}\lambda} \mathcal{G}(\vec{q}\lambda) \hat{\epsilon}_i(\vec{q}\lambda) e^{i\vec{q}\cdot\vec{r}}, \quad (13)$$

where the sum on λ ranges over the three polarization directions (one longitudinal, and two transverse) associated with each wave vector \vec{q} . If this form is substituted into Eq. (12), and the result is multiplied by $e^{-i\vec{k}\cdot\vec{r}}$ and then both sides are integrated over the crystal volume, one has

$$\begin{aligned} \sum_{\lambda} \mathcal{G}(\vec{k}\lambda) \left\{ \left[(k^2 + K^2) \left(k^2 - \frac{\Omega^2}{c^2} \epsilon_0 \right) + \frac{4\pi\Omega^2 \chi_L}{\alpha^2 c^2} \right] \epsilon_i(\vec{k}\lambda) \right. \\ \left. - (k^2 + K^2) [\vec{k} \cdot \hat{\epsilon}(\vec{k}\lambda)] k_i \right\} \\ = -\frac{\Omega^2}{c^2} \sum_{\vec{q}\lambda} M(\vec{k}, \vec{q}) \hat{\epsilon}(\vec{q}\lambda) \mathcal{G}(\vec{q}\lambda), \end{aligned} \quad (14)$$

where we have defined

$$\begin{aligned} M(\vec{k}, \vec{q}) = \int \frac{d^3r}{V} \left(-(k^2 + K^2)\Delta\epsilon_0(\vec{r}) \right. \\ \left. + \frac{4\pi\Delta\chi_L(\vec{r})}{\alpha^2} \right) e^{-i(\vec{k}-\vec{q})\cdot\vec{r}}. \end{aligned} \quad (15)$$

We now multiply Eq. (14) by $\epsilon_i(\vec{k}\lambda')$ and note the orthogonality property

$$\sum_i \hat{\epsilon}_i(\vec{k}\lambda) \hat{\epsilon}_i(\vec{k}\lambda') = \delta_{\lambda\lambda'}, \quad (16)$$

to obtain an equation for $\mathcal{G}(\vec{k}\lambda)$:

$$\begin{aligned} M(\vec{k}, \vec{q}) = \frac{1}{V} \sum_n V_n \left(-(k^2 + K^2)\Delta\epsilon_0^{(n)} \right. \\ \left. + 4\pi\Delta\chi_L^{(n)}/\alpha^2 \right) \times F_n(\vec{Q}) e^{i\vec{Q}\cdot\vec{R}_n}, \end{aligned} \quad (18)$$

where V_n is the volume of the n th defect, and $F_n(\vec{Q})$ is a form factor defined by

$$F_n(\vec{Q}) = \int \frac{d^3\rho}{V_n} e^{i\vec{Q}\cdot\vec{\rho}}, \quad (19a)$$

where the integration ranges over the volume of the defect, with the origin located at \vec{R}_n . Notice that independent of the shape of the defect, $F_n(0) = 1$.

For a spherical defect of radius R_0 , one has

$$F(Q) = \frac{3}{(QR_0)^3} (\sin QR_0 - QR_0 \cos QR_0). \quad (19b)$$

If we recall the definition of $\epsilon(\vec{k}, \Omega)$, and define

$$\Delta\epsilon^{(n)}(\vec{k}, \Omega) = \Delta\epsilon_0^{(n)} + \frac{4\pi\Delta\chi_L^{(n)}\omega_{TQ}^2}{\omega_{TQ}^2(k) - \Omega^2}, \quad (20)$$

then Eq. (17) becomes

$$\begin{aligned} \mathcal{G}(\vec{k}\lambda) &= \frac{\Omega^2}{c^2} \frac{1}{k^2(1 - \delta_{\lambda, \ell}) - (\Omega^2/c^2)\epsilon(\vec{k}, \Omega)} \\ &\times \sum_{\alpha'} \frac{V_\pi}{V} \Delta\epsilon^{(n)}(\vec{k}, \Omega) \\ &\times \sum_{\vec{q}} F_n(\vec{q}) e^{i\vec{q} \cdot \vec{R}_n} \hat{\epsilon}(\vec{k}\lambda') \cdot \hat{\epsilon}(\vec{q}\lambda') \mathcal{G}(\vec{q}\lambda'). \end{aligned} \quad (21)$$

Equation (21) is in fact an integral equation for the amplitude $\mathcal{G}(k\lambda)$. To generate the Born series of scattering theory, one may solve Eq. (21) by an iterative method, using for the zero-order solution a plane wave of the appropriate polarization. In the language of Eq. (21), in zero order one has

$$\mathcal{G}(q\lambda') = \mathcal{E}_0 \delta_{i\vec{k}_0} \delta_{\lambda_0}, \quad (22)$$

where \vec{k}_0 is the wave vector of the incident wave, and λ_0 its polarization.

We shall study the scattering produced by a single very small void placed at the origin of the coordinate system, in the first Born approximation. For a point defect, the form factor may be replaced by unity, and the zero-order form for $\mathcal{G}(\vec{q}\lambda)$ given in Eq. (22) generates the first Born approximation, when inserted into the right-hand side of Eq. (22). For a void, $\Delta\epsilon(\vec{k}, \Omega) = 1 - \epsilon(\vec{k}, \Omega)$.

With these approximations, the amplitude $\vec{E}^{(s)}(\vec{r})$ of the scattered field is found to be

$$\begin{aligned} \vec{E}^{(s)}(\vec{r}) &= \frac{V_0 \mathcal{E}_0}{8\pi^3} \sum_{\lambda} \int d^3k e^{i\vec{k} \cdot \vec{r}} \\ &\times \hat{\epsilon}(k\lambda) [\hat{\epsilon}(\vec{k}\lambda) \cdot \hat{\epsilon}(\vec{k}_0\lambda_0)] \\ &\times \frac{\Omega^2 [\epsilon(k, \Omega) - 1]}{\Omega^2 \epsilon(k, \Omega) - c^2 k^2 (1 - \delta_{\lambda, i})}, \end{aligned} \quad (23)$$

where V_0 is the volume of the void.

Through use of the identity

$$\sum_{\lambda} \hat{\epsilon}_i(k\lambda) \hat{\epsilon}_j(k\lambda) = \delta_{ij},$$

and the fact that $\hat{\epsilon}(\vec{k}l) = \hat{k}$, the result in Eq. (23) may be written

$$\vec{E}^{(s)}(\vec{r}) = \vec{E}^{(l)}(\vec{r}) + \vec{E}^{(t)}(\vec{r}),$$

where

$$\begin{aligned} E_i^{(l)}(\vec{r}) &= -\frac{\mathcal{E}_0 V_0}{8\pi^3} \sum_j \hat{\epsilon}_j(\vec{k}_0\lambda_0) \frac{\partial^2}{\partial x_i \partial x_j} \\ &\times \int \frac{d^3k}{k^2} \frac{e^{i\vec{k} \cdot \vec{r}}}{\epsilon(k, \Omega)}, \end{aligned} \quad (24a)$$

and

$$\begin{aligned} E_i^{(t)}(\vec{r}) &= -\frac{\mathcal{E}_0 V_0}{8\pi^3} \sum_j \hat{\epsilon}_j(k_0\lambda_0) \left(\delta_{ij} \nabla^2 - \frac{\partial^2}{\partial x_i \partial x_j} \right) \\ &\times \int \frac{d^3k}{k^2} \left(\frac{k^2 - \Omega^2/c^2}{k^2 - (\Omega^2/c^2)\epsilon(k, \Omega)} \right) e^{i\vec{k} \cdot \vec{r}}. \end{aligned} \quad (24b)$$

The contribution to the scattered field from Eq. (24a) is the portion carried by the longitudinal mode (the mode of wave vector k_3 in Fig. 1). One can see this since the pole of the integrand comes from the zero of $\epsilon(k, \Omega)$. The contribution from Eq. (24b) contains the contribution from the two transverse polaritons of frequency Ω (the modes with wave vectors k_1 and k_2 in Fig. 1). All three modes transport energy away from the defect only if the frequency Ω of the incident wave lies below the maximum in the lower transverse polariton branch. One has several possibilities:

(a) The frequency of the incident wave (either transversely or longitudinally polarized) lies below the maximum frequency ω_M of the lower polariton branch. Then all three modes propagate, and carry energy away from the defect.

(b) The frequency of the incoming wave lies in the range $\omega_M < \Omega < \omega_{LO}$. Then the incoming wave must be a longitudinal wave, since no propagating wave of transverse character exists in this frequency region. The only propagating mode in the final state is also a longitudinal mode; this is the only polarization that carries energy away from the defect. There is a disturbance of transverse polarization induced around the defect, but its magnitude drops to zero exponentially as one moves away from the defect. [The zeros of $c^2 k^2 - \Omega^2 \epsilon(k, \Omega)$ lie on the imaginary axis in this frequency region.]

(c) The frequency of the incident (transverse) polariton lies above ω_{LO} . Then there is one propagating transverse mode in the final state, and the remaining contributions to the scattered field decay to zero exponentially as one moves away from the defect. [The zero of $\epsilon(k, \Omega)$ lies on the imaginary axis, while one zero of $c^2 k^2 - \Omega^2 \epsilon(k, \Omega)$ lies on the real axis and one in the imaginary axis.]

The contour integration in Eq. (24a) is readily performed to yield the very simple result

$$\begin{aligned} E_i^{(l)}(\vec{r}) &= \frac{\mathcal{E}_0 V_0}{2\pi k_1 (\partial\epsilon/\partial k)_1} \\ &\times \sum_j \hat{\epsilon}(k_0\lambda_0) \frac{\partial^2}{\partial x_i \partial x_j} \frac{e^{ik_1 r}}{r}, \end{aligned} \quad (25)$$

where k_1 is the wave vector (possibly imaginary) where $\epsilon(k_1, \Omega) = 0$. For frequencies below ω_{LO} , where k_1 is real, after some rearrangement, in the radiation zone far from the defect, Eq. (25) may be written

$$\vec{E}^{(t)}(\vec{r}) = + \frac{\mathcal{G}_0 V_0}{4\pi} \frac{\epsilon_s - \epsilon_0}{\alpha^2 \epsilon_0^2} \frac{e^{ikr}}{r} \hat{n} [\hat{n} \cdot \hat{\epsilon}(k_0 \lambda_0)], \quad (26)$$

where ϵ_s is the static dielectric constant at $k=0$, and \hat{n} is a vector from the origin to the observation point.

For transverse waves, one finds

$$\begin{aligned} E_i^{(t)}(\vec{r}) = & - \frac{\mathcal{G}_0 V_0}{2\pi} \left(\frac{\Omega}{c} \right)^2 \\ & \times \sum_t \left\{ \left[\epsilon(k_t, \Omega) - 1 \right] / k_t \left[2k_t - \left(\frac{\Omega}{c} \right)^2 \frac{\partial \epsilon}{\partial k} \Big|_{k_t} \right] \right\} \\ & \times \left(\delta_{ij} \nabla^2 - \frac{\partial^2}{\partial x_i \partial x_j} \right) \frac{e^{ik_t r}}{r}. \end{aligned} \quad (27)$$

The sum includes the two wave vectors k_t for which $c^2 k_t^2 = \Omega^2 \epsilon(k_t, \Omega)$. For frequencies below the maximum ω_M of the lower polariton branch, both values of k_t are real. Then far from the defect, Eq. (27) becomes

$$\begin{aligned} \vec{E}^{(t)}(\vec{r}) = & \frac{\mathcal{G}_0 V_0}{2\pi} \left(\frac{\Omega}{c} \right)^2 \left\{ \hat{\epsilon}(\vec{k}_0 \lambda_0) - [\hat{n} \cdot \hat{\epsilon}(k_0 \lambda_0)] \hat{n} \right\} \\ & \times \sum_t \left\{ \left[\epsilon(k_t, \Omega) - 1 \right] / k_t \left[2k_t - \left(\frac{\Omega}{c} \right)^2 \frac{\partial \epsilon}{\partial k} \Big|_{k_t} \right] \right\} \\ & \times \frac{e^{ik_t r}}{r}. \end{aligned} \quad (28)$$

From the expressions for the amplitudes of the scattered fields given in Eqs. (26) and (28), we construct expressions for the scattering cross section. The Poynting vector gives the energy/(unit time) (unit area) carried by a wave. In the Appendix, we derive the form of the Poynting vector \vec{S} for our model. In the presence of spatial dispersion, we find

$$\vec{S} = \vec{S}_E + \vec{S}_M, \quad (29)$$

where $\vec{S}_E = (c/4\pi) \vec{E} \times \vec{H}$ is the Poynting vector of electromagnetic theory, and \vec{S}_M is a contribution to \vec{S} from the energy transported by the excitation in the medium. For \vec{S}_M we find for our model

$$S_{Mj} = \frac{4\pi \alpha^2 \omega_T^2}{\omega_p^2} \vec{P} \cdot \frac{\partial \vec{P}}{\partial x_j}. \quad (30)$$

where S_{Mj} is the j th Cartesian component of \vec{S}_M .

For a plane wave, the Poynting vector becomes (in magnitude)

$$S = \frac{c |\vec{E}|^2}{8\pi} \left(\epsilon^{1/2}(k, \omega) - \frac{1}{2} \frac{\omega}{2c} \frac{\partial \epsilon(k, \omega)}{\partial k} \right). \quad (31)$$

Thus, if we calculate the scattered energy per unit time which flows through a sphere of very large radius R , we have, for the transverse and longitudinal waves, respectively,

$$\frac{dU_t^{(s)}}{dt} = \frac{e |\mathcal{G}_0|^2 V_0^2}{8\pi (4\pi)^2} \left(\frac{\Omega}{c} \right)^4 \left[\epsilon(k_t, \Omega) |\epsilon(k_t, \Omega) - 1|^2 / \right.$$

$$\left. \left| \epsilon^{1/2}(k_t, \Omega) - \frac{1}{2} \frac{\Omega}{c} \frac{\partial \epsilon}{\partial k} \Big|_{k_t} \right| \right] \times \int d\Omega(\hat{n}) \{1 - [\hat{n} \cdot \hat{\epsilon}(k_0 \lambda_0)]^2\} \quad (32)$$

and

$$\begin{aligned} \frac{dU_l^{(s)}}{dt} = & \frac{\Omega |\mathcal{G}_0|^2 V_0^2}{16\pi (4\pi)^2} \frac{\partial \epsilon}{\partial k}(k_l, \Omega) \frac{(\epsilon_s - \epsilon_0)^2}{\alpha^4 \epsilon_0^4} \\ & \times \int d\Omega(\hat{n}) |\hat{n} \cdot \hat{\epsilon}(k_0 \lambda_0)|^2 \end{aligned} \quad (33)$$

We define scattering efficiencies by dividing Eqs. (32) and (33) by the energy/(unit time) incident on the defect. If A_0 is the cross-sectional area of the defect normal to the direction of the incident wave, then the energy/(unit time) incident on the defect is

$$\begin{aligned} \frac{dU_I}{dt} = & A_0 S_I \\ = & A_0 \left(\epsilon^{1/2}(k_I, \Omega) - \frac{\Omega}{2c} \frac{\partial \epsilon(k_I, \Omega)}{\partial \Omega} \right) \frac{|\mathcal{G}_0|^2}{8\pi}. \end{aligned}$$

Note that the value of the angular integrals in Eqs. (32) and (33) are independent of the polarization λ_0 of the incident wave. The integrals have the value $8\pi/3$ and $4\pi/3$, respectively. Then for the scattering efficiencies f_l and f_t of the longitudinal and transverse waves one has

$$\begin{aligned} f_t = & \frac{V_0^2}{6\pi A_0} \left(\frac{\Omega}{c} \right)^4 \left(\epsilon(k_t, \Omega) |\epsilon(k_t, \Omega) - 1|^2 / \right. \\ & \left. \left| \epsilon^{1/2}(k_t, \Omega) - \frac{\Omega}{2c} \frac{\partial \epsilon}{\partial k}(k_t, \Omega) \right| \right. \\ & \left. \times 1 / \left| \epsilon^{1/2}(k_I, \Omega) - \frac{\Omega}{2c} \frac{\partial \epsilon}{\partial k}(k_I, \Omega) \right| \right), \end{aligned} \quad (34)$$

and

$$\begin{aligned} f_l = & \frac{\Omega V_0^2}{24\pi A_0} \frac{\partial \epsilon}{\partial k}(k_l, \Omega) \frac{(\epsilon_s - \epsilon_0)^2}{\alpha^4 \epsilon_0^4} \\ & \times 1 / \left| \epsilon^{1/2}(k_I, \Omega) - \frac{\Omega}{2c} \frac{\partial \epsilon}{\partial k}(k_I, \Omega) \right|. \end{aligned} \quad (35)$$

The results in Eqs. (34) and (35) are the principal results of the present paper. Notice that a necessary assumption in their derivation is the replacement of the form factor $F(\vec{Q})$, defined in Eq. (19), by unity. This means that the results are valid only if the wavelengths of all waves involved in the scattering process (including the waves k_2 and k_3 of Fig. 1) are large compared to the linear dimensions of the defect. We shall base the numerical calculations of Sec. III on these results.

We conclude the present section by displaying the scattering efficiency f_0 for scattering from a defect, in the absence of spatial dispersion.³ The results appropriate to this case may be obtained from Eq. (34) by letting $\epsilon(k, \Omega) \rightarrow \epsilon_0(\Omega)$, the dielectric constant of the material when $\alpha^2 = 0$. This gives

$$f_0 = \frac{V_0^2}{6\pi A_0} \left(\frac{\Omega}{c}\right)^4 |\epsilon_0(\Omega) - 1|^2, \quad (36)$$

which for a spherical defect of radius R_0 becomes

$$f_0 = \frac{2}{27} R_0^4 \frac{\Omega}{c} |\epsilon_0(\Omega) - 1|^2. \quad (37)$$

III. NUMERICAL CALCULATIONS OF THE SCATTERING EFFICIENCY

In this section we present a numerical study of the scattering efficiency of a polariton from a point defect. In the calculations reported below, we normalize the scattering efficiencies f_i and f_t of Sec. II by dividing them by the value f_0 [Eq. (36)] appropriate to the case where spatial dispersion is absent. Thus, we study the quantities

$$r_i = f_i/f_0 \quad (38)$$

and

$$r_t = f_t/f_0. \quad (39)$$

We also assume that the incident wave is a transverse wave with frequency below the maximum frequency ω_M of the lowest transverse polariton branch in Fig. 1. We have chosen parameters characteristic of the TO phonon in GaP, i. e., $\omega_{TO} = 367 \text{ cm}^{-1}$, while ϵ_s and ϵ_0 assume the values of 10.18 and 8.46, respectively. The only parameter which remains is α , which is a measure of the curvature of the TO-phonon branch at $k=0$. Inspection of the optical phonon branch of the simple diatomic chain⁶ shows that the order of magnitude of α_0^{-1} , where a_0 is the lattice constant. For the calculations reported here, we have chosen the value $\alpha \approx 10^8$ as a rough estimate.

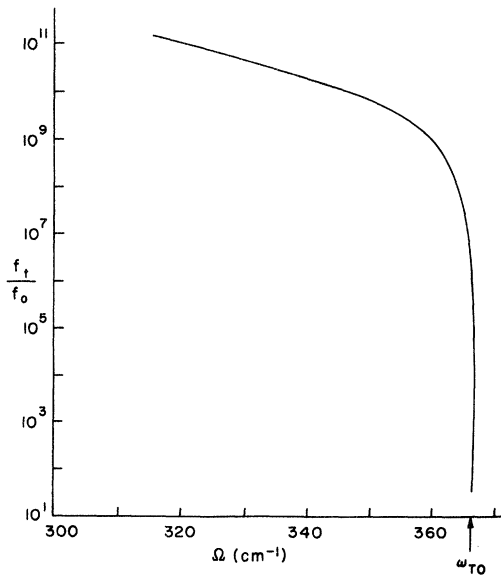


FIG. 2. Ratio f_t/f_0 for the TO-phonon polariton in GaP. The parameters employed in the calculation are described in the text.

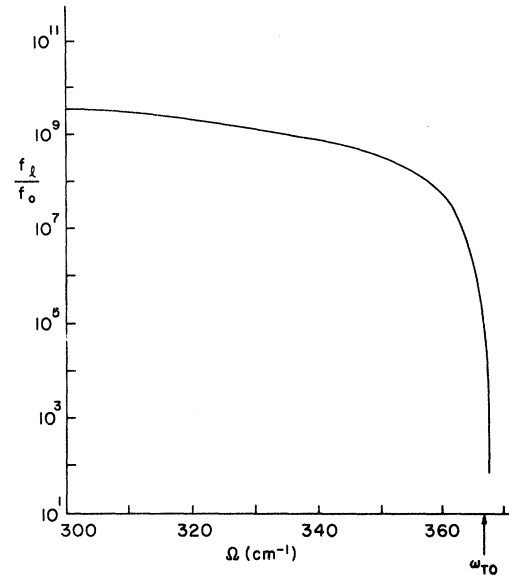


FIG. 3. Ratio f_i/f_0 for the TO-phonon polariton in GaP. The parameters employed in the calculation are described in the text.

First consider the behavior of r_t , defined in Eq. (39). As one sees in Fig. 1, for each incident wave with frequency less than ω_M , there are two final-state transverse polaritons, with wave vector k_1 and k_2 , respectively. The state k_1 lies to the left of the state with wave vector k_M that has frequency ω_M , while the state k_2 lies to the right. We denote these two contributions to r_t by $r_t^{(1)}$ and $r_t^{(2)}$, respectively.

In the absence of spatial dispersion, the quantity $r_t^{(1)}$ reduces to unity. We find that for the parameters described above, $r_t^{(1)}$ is very close to unity for the whole range of frequencies explored (300–366.7 cm^{-1}) except for frequencies very close (within 1 cm^{-1}) of ω_{TO} , where $r_t^{(1)}$ begins to increase very rapidly as Ω approaches ω_M . Thus, the effect of spatial dispersion on the contribution to r_t from scattering into final states of type k_1 in Fig. 1 is very small, for all frequencies of interest. This is what one would expect from physical considerations.

In Fig. 2, we show the behavior of $r_t^{(2)}$, in the frequency range from 300 to 366.7 cm^{-1} . This quantity is very large compared to unity, and it begins to decrease rapidly as Ω increases toward ω_M , where it must join smoothly on to $r_t^{(1)}$. In Fig. 3, we show the behavior of r_i . This quantity is very large compared to unity also, although it is smaller by one to two orders of magnitude than $r_t^{(2)}$.

These calculations show that in the presence of spatial dispersion, the rate for scattering of a polariton from a point defect is dominated by scattering into the large wave vector states of the type k_2 and k_3 in Fig. 1. Indeed, in the frequency range

where such states are allowed, the cross section is enhanced by many orders of magnitude over the value appropriate to the Rayleigh scattering of a simple electromagnetic wave from the defect [Eqs. (36) and (37)].

The physical origin of this behavior lies in two effects.⁷ First of all, to use quantum-mechanical language, the matrix element for coupling into a final state of large wave vector is very big. Second, the number of final states available is very much larger for states of type k_2 or k_3 , compared to k_1 . These two factors outweigh the fact that the energy transport velocity is small in the final state, so these waves transfer energy away from the defect inefficiently.

The calculations above show that the availability of final states with large wave vectors leads to a very large enhancement of the cross section for defect scattering. We conclude with an estimate of the polariton mean free path.

If there are n defects per unit volume, and the cross-sectional area of each defect is A_0 , then the mean free path l of the polariton is

$$1/l = nA_0f, \quad (40)$$

where

$$f = f_1 + \sum_i f_i \quad (41)$$

is the total scattering efficiency. If V_0 is the volume of the unit cell of the crystal, and the defect concentration is c , then $n = c/V_0$. Thus we have

$$l = (V_0/A_0)(1/cf). \quad (42)$$

The ratio V_0/A_0 is the order of the lattice constant a_0 , so for the mean free path in units of the lattice constant we have

$$l/a_0 \approx 1/cf. \quad (43)$$

For a polariton in GaP with a frequency of 340 cm^{-1} , we estimate $f_0 \approx 5 \times 10^{-16}$. The calculations in Figs. 2 and 3 than show $f \approx 5 \times 10^{-6}$. Thus, even for a large concentration of microscopic defects ($c = 0.1$, say), the mean free path of the polariton is quite macroscopic, on the order of one millimeter. Thus, even in the presence of the very large enhancement of the cross section produced by spatial dispersion effects, the mean free path of the polariton is so long that it is hard to imagine that scattering of polaritons from microscopic defects can influence the shape of the Raman line. Thus, as remarked in Sec. I, the present calculation reinforces the conclusions reached by Evans and Ushioda that the anomalous line shapes observed by them have their origin in macroscopic strains.

The notion that the scattering rate for defect scattering receives its largest contribution from states of large wave vector accessible by virtue of spatial

dispersion effects is applicable to exciton polaritons, as well as the TO-phonon polaritons described here. However, while methods similar to those described here may be applied in the exciton regime, the interaction of an exciton-polariton with the defect will be more complex than that envisioned in our simple model. Thus, one would need to examine pictures of exciton-defect interactions in detail, and combine this with a calculation which proceeds as we do here.

APPENDIX: SOME PROPERTIES OF THE MODEL DIELECTRIC IN THE PRESENCE OF SPATIAL DISPERSION

Consider first the energy density in the material. In the absence of spatial dispersion, the total energy density in the material is given by the well-known form⁴

$$U = U_E + U_M, \quad (A1)$$

where

$$U_E = (1/8\pi)(\epsilon_0 E^2 + H^2) \quad (A2)$$

and

$$U_M = \frac{1}{2} n M \dot{u}^2 + \frac{1}{2} n M \omega_{TO}^2 u^2, \quad (A3)$$

where the notation is the same as in the text. If we rewrite U_M so that it is expressed in terms of the electric dipole-moment density P , and add to U_M the term in $|\nabla \vec{P}|^2$ present when spatial dispersion is present, Eq. (A3) becomes

$$U_M = \frac{2\pi}{\omega_P^2} \dot{P}^2 + \frac{2\pi\omega_{TO}^2}{\omega_P^2} P^2 - \frac{2\pi\alpha^2\omega_{TO}^2}{\omega_P^2} |\nabla \vec{P}|^2. \quad (A4)$$

We may derive an expression for the Poynting vector by computing $\partial U / \partial t$, and then utilizing the equations of motion in Sec. II of the text to write the result in the form

$$\frac{\partial U}{\partial t} + \nabla \cdot \vec{S} = 0 \quad (A5)$$

One finds the Poynting vector \vec{S} has the form

$$\vec{S} = \vec{S}_E + \vec{S}_M, \quad (A6)$$

where

$$\vec{S}_E = (c/4\pi) \vec{E} \times \vec{H} \quad (A7)$$

is the Poynting vector of electromagnetic theory, and the i th Cartesian component of S_M^i is given by

$$S_M^i = \frac{4\pi\alpha^2\omega_{TO}^2}{\omega_P^2} \vec{P} \cdot \frac{\partial \vec{P}}{\partial x_i}. \quad (A8)$$

It is interesting to use the above results to compute the energy transport velocity $V_E(\omega, k)$ of a polariton of frequency ω and wave vector k , following a method used by Loudon,⁵ in the absence of spatial dispersion.

The energy transport velocity (always parallel to \vec{k} for our isotropic model) is defined by the relation

$$\langle S \rangle = V_E \langle U \rangle,$$

where $\langle S \rangle$ and $\langle U \rangle$ are the time averages of the Poynting vector and energy density, respectively. An explicit calculation shows that

$$\langle S \rangle = \frac{c |E_0|^2}{8\pi} \left(\epsilon(k, \Omega)^{1/2} - \frac{\Omega}{2c} \frac{\partial \epsilon(k, \Omega)}{\partial k} \right), \quad (\text{A9})$$

where the term $\partial \epsilon / \partial k$ has its origin in the presence of \vec{S}_M in Eq. (A6) and E_0 is the amplitude of the electric field in the wave. For $\langle U \rangle$, one has an expression quite similar to that obtained in the absence of spatial dispersion⁴:

$$\langle U \rangle = \frac{|E_0|^2}{8\pi} \left(\epsilon(k, \Omega) + \frac{\Omega}{2} \frac{\partial \epsilon(k, \Omega)}{\partial \Omega} \right), \quad (\text{A10})$$

so that

$$\frac{V_E(k, \Omega)}{c} = \left(\epsilon(k, \Omega)^{1/2} - \frac{\Omega}{2c} \frac{\partial \epsilon(k, \Omega)}{\partial k} \right) \left(\epsilon(k, \Omega) + \frac{\Omega}{2} \frac{\partial \epsilon(k, \Omega)}{\partial \Omega} \right). \quad (\text{A11})$$

It is straightforward to verify that the energy transport velocity $V_E(k, \Omega)$ is identical to the group velocity

$$V_g(k, \Omega) = \partial \Omega(k) / \partial k \quad (\text{A12})$$

calculated from the dispersion relation

$$c^2 k^2 / \Omega^2 = \epsilon(k, \Omega).$$

*Research sponsored by the Air Force Office of Scientific Research, Office of Aerospace Research, U.S.A.F. under Grant No. AFOSR 71-2018.

¹See the discussions in V. M. Agranovich and V. L. Ginzburg, *Spatial Dispersion in Crystal Optics and the Theory of Excitons* (Interscience, London, 1966). See also the more recent references cited in A. A. Maradudin and D. L. Mills, Phys. Rev. B 7, 2787 (1973).

²D. J. Evans and S. Ushioda, Phys. Rev. B 9, 1638 (1974).

³Only final states of the type k_1 in Fig. 1 contribute to the cross section in the limit $\alpha^2 \rightarrow 0$. (To recover the correct form of the contribution from final states k_2 and k_3 as $\alpha^2 \rightarrow 0$, the full form of the form factor in Eq. (19a) must be retained.)

⁴L. Brillouin, *Wave Propagation and Group Velocity* (Academic, New York, 1960).

⁵R. Loudon, J. Phys. A 3, 233 (1970).

⁶For example, see C. Kittel, *Introduction to Solid State Physics*, 4th ed. (Wiley, New York, 1971), Chap. 5.

⁷This is true when the wavelength of both the wave in the initial and final states are large compared to the size of the defect. We have assumed this is the case in our calculations. When k_2 or k_3 become so large that this is not true, one must include the effect of the form factor, which falls off rapidly as its argument approaches infinity, as one sees from Eq. (19b). Thus, our calculations provide an upper limit for scattering from a defect of finite size.